Designing ternary superconducting hydrides with A15-type structure at moderate pressures

Xudong Wei,[1] Xiaokuan Hao,[1] Aitor Bergara,[2,3,4] Eva Zurek,[5] Xiaowei Liang,[1] Linyan Wang,[1] Xiaoxu Song,[1] Peifang Li,[6] Lin Wang,[1] Guoying Gao,[1,] and Yongjun Tian[1]*

[1]*Center for High Pressure Science (CHiPS), State Key Laboratory of Metastable Materials Science and Technology, Yanshan University, Qinhuangdao, Hebei, 066004, China*
[2]*Physics Department and EHU Quantum Center, University of the Basque Country, UPV/EHU, 48080 Bilbao, Spain*
[3]*Donostia International Physics Center (DIPC), 20018 Donostia, Spain*

[4]*Centro de Física de Materiales CFM, Centro Mixto CSIC-UPV/EHU, 20018 Donostia, Spain*
[5]*Department of Chemistry, State University of New York at Buffalo, Buffalo, New York 14260-3000, United States*
[6]*Extreme Conditions Physics Research Team, College of Mathematics and Physics, Inner Mongolia Minzu University, Tongliao 028043, China*

**Corresponding author:*
E-mail address: gaoguoying@ysu.edu.cn (*Guoying Gao*)

Abstract

Ever since hydrogen-based superconductors have been actively considered as candidates for room-temperature superconductors, binary hydrides have been almost completely explored theoretically. Now researchers are turning their interest to ternary hydrides. However, the enormous compositional and structural possibilities in the ternary hydride space limit the search efficiency. Here, using an advanced crystal structure search method combined with first-principles calculations, a series of ternary hydrides AXH_6 ($MgPH_6$, $MgAsH_6$, $CaSbH_6$, $CaSnH_6$, $NaSbH_6$ and $ScSiH_6$) with the A15 structure are predicted to be stable at around one million atmospheres. Among them, $CaSnH_6$ presents the lowest thermodynamically stable pressure of 110 GPa and $CaSbH_6$, $CaSnH_6$ and $ScSiH_6$ may be dynamically stable down to 41, 71 and 85 GPa, respectively. Hydrogen atoms in these A15-type structures are found to form weak covalent bonds to X atoms. More interestingly, we find that ternary hydrides with the AXH_6 stoichiometry may assume the A15-type structure under pressure when the sum of the chemical valences of the two non-hydrogen atoms is six or seven. Based on electron-phonon coupling calculations, all these ternary hydrides are estimated to be superconductors. $CaSbH_6$, $CaSnH_6$ and $ScSiH_6$ have T_cs of 65, 53 and 116 K at 45, 75 and 90 GPa, respectively, while $MgPH_6$ has the highest T_c of 148 K at 135 GPa. Our study will provide guidance for designing high T_c ternary hydrides near ambient pressures.

Keywords: Superconductivity; Ternary hydrides; A15-type structure; Electron-phonon coupling; Low pressures.

1. Introduction

Many A_3B compounds crystalize in the simple cubic $Pm\bar{3}n$ structure (Z=2, Pearson symbol *cP*6), which is usually called the A15 structure. V_3Si was the first superconductor synthesized with the A15 structure [1]. Since then, different A15-family superconductors (e.g., Nb_3Ge, Nb_3Sn, V_3Ga and other niobium compounds) have been extensively investigated both theoretically and experimentally [2-6]. As it is well known, A15 Nb_3Ge films held the record for the highest T_c of 23.2 K [2, 3] before Bednorz *et al*. made a breakthrough discovery in layered $(La, Ba)_2CuO_4$ compound, with a T_c of ~35 K [7]. In 2008 Ganin *et al*. synthesized A15 Cs_3C_{60} and observed that it became superconducting under pressure and its T_c reached 38 K at ~7 kbar [8].

For binary hydrides, α-UH_3 was synthesized in 1954 and found to crystallize in the A15 structure [9]. Later, in 2007, AlH_3 was first predicted and then found to adopt the A15 structure above 100 GPa [10, 11]. However, no superconductivity was observed down to 4 K [11]. In 2011 we predicted the A15 structure for gallane (GaH_3) above 160 GPa, which was calculated to possess a high T_c of 86 K at 160 GPa and increases to 102 K at 120 GPa [12]. Recently, Xie *et al*. synthesized the A15 ZrH_3 from ZrH_2+H_2 at 30.4 GPa and 300 K or from Zr+H_2 at 47 GPa and 1500 K [13]. Currently, some other trihydrides have also been predicted and synthesized with a distorted A15 structure [14-16]. For example, in 2013, we predicted a body-centered cubic $I\bar{4}3d$ structure (Z = 16, Pearson symbol *cI*64) for NbH_3 above 33 GPa [14]. This phase is the well-known Domeykite mineral Cu_3As arrangement, which can be also seen as a distorted A15 structure. Four years later, we successfully synthesized NbH_3 with the same structure from Nb and hydrogen under high pressure and high temperature [15]. Unfortunately, we did not explore its superconductivity experimentally at that time. With the same group as Nb, Ta trihydrides (TaH_3) were also synthesized with the same $I\bar{4}3d$ structure and predicted to be superconducting with a T_c of 23 K at 80 GPa [16, 17].

For ternary hydrides, Ma *et al*. first predicted that $MgSiH_6$ [18]and $MgGeH_6$ [19] are stable in the $Pm\bar{3}$ structure, which is similar to the A15. The only difference is that the Mg and Ge atoms together form the body-centered cubic lattice. $MgSiH_6$ and $MgGeH_6$ are also predicted to be superconductors with a T_c of 63 and 67 K at 250 and

200 GPa, respectively. Later, Shao *et al*. predicted the same $Pm\bar{3}$ structure for $LiPH_6$, whose T_c reached as high as 167 K at 200 GPa [20]. Therefore, including two elements with hydrogen in the A15 structure seems to enhance T_c under pressure. However, it is not yet known whether ternary hydrides with an A15 structure can be stable at around a million atmospheres or even at much lower pressures, while keeping their high T_cs.

Here, we computationally designed a series of ternary hydrides ($MgPH_6$, $MgAsH_6$, $CaSbH_6$, $CaSnH_6$, $NaSbH_6$ and $ScSiH_6$), which can be stable in the A15-type structure under pressure. Interestingly, four of these hydrides are thermodynamically stable at much lower pressures than the previously predicted $LiPH_6$, $MgSiH_6$ and $MgGeH_6$. All these hydrides are also dynamically stable at lower pressures, and three of them can even be stable below one million atmospheres. Chemical bonding analysis suggests that all of these A15-type hydrides contain XH_{12} units. Together with the previously predicted $LiPH_6$, $MgSiH_6$ and $MgGeH_6$, we have found that in these ternary hydrides with stable A15-type structure, the sum of the chemical valence of the two non-hydrogen elements is six or seven. Electron-phonon coupling (EPC) calculations show that all of these ternary hydrides are superconductors with T_cs of 65, 53 and 116 K at 45, 75 and 90 GPa, for $CaSbH_6$, $CaSnH_6$ and $ScSiH_6$, respectively.

2. Computational details

Starting from A15 GaH_3 as the matrix structure, structural replacements were made for AXH_6 (A= Li, Na, K, Rb, Cs, Mg, Ca, Sr, Ba, Sc, Y and X= Si, Ge, Sn, Pb, P, As, Sb, Bi, S, Se, Te). Crystal structure prediction calculations were also performed using the particle swarm optimization technique implemented in the CALYPSO code [21, 22] in a pressure range of 50-300 GPa. The structural relaxation and electronic structure calculations were performed in the framework of density functional theory using the Perdew-Burke-Ernzerhof generalized gradient approximation method as implemented in the Vienna ab initio simulation package [23, 24]. The projector-augmented wave method was used, where $2s^2 2p^6 3s^2$, $3p^6 4s^2$, $2p^6 3s^1$, $3s^2 3p^6 4s^2 3d^1$, $3s^2 3p^2$, $5s^2 5p^2$, $3s^2 3p^3$, $4s^2 4p^3$, $5s^2 5p^3$ and $1s^1$ are treated as valence electrons for Mg, Ca, Na, Sc, Si, Sn, P, As, Sb and H, respectively[25]. A plane wave energy cutoff of 600 eV and appropriate MonkhorstPack *k*-meshes were chosen to ensure that enthalpy calculations were converged to less than 1 meV/atom. Phonon calculations were performed using the supercell method or density functional perturbation theory (DFPT) with PHONOPY [26] and the Quantum-ESPRESSO (QE) codes[27], respectively. Further EPC calculations were performed using DFPT, as implemented in the QE package[27], where ultrasoft pseudopotentials for Mg, Ca, Na, Sc, Si, Sn, P, As, Sb and H were employed with a kinetic energy cutoff of 80-100 Ry. 8×8×8 *q*-meshes were used in the EPC calculations for $Pm\bar{3}$ AXH_6. The critical temperature T_cs were estimated using the Allen-Dynes modified McMillan equation[28] and by numerically solving the Eliashberg equations[29] for ternary hydrides, when lambda is less than 1.5 and larger than 1.5, respectively.

3. Results and discussion

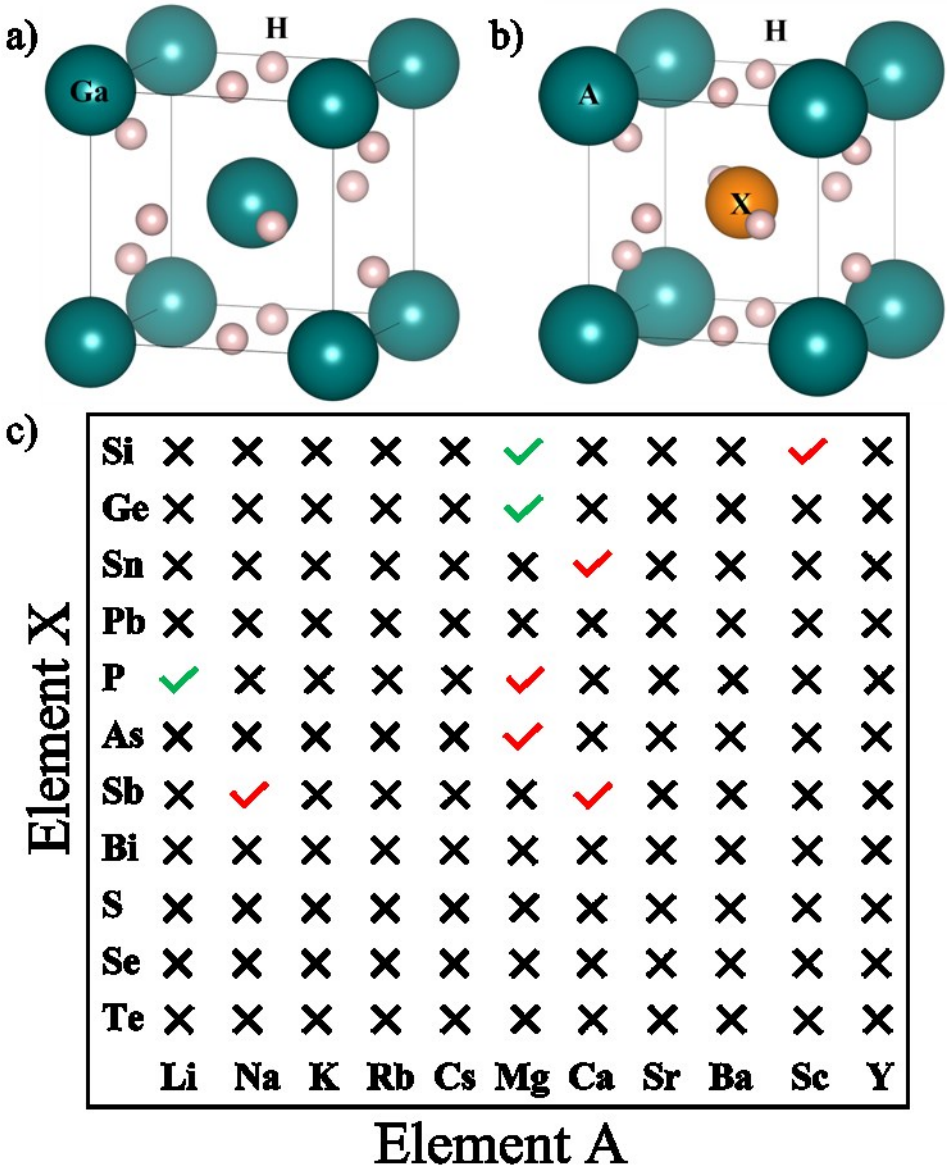

Figure 1: a) $Pm\bar{3}n$ (A15) GaH_3. Turquoise and light pink spheres represent Ga and H atoms, respectively. b) $Pm\bar{3}$ AXH_6. A and X atoms are located at the vertices and centre of the bcc lattices. c) Schematic diagram of thermodynamic stability for various A and X elements in the AXH_6 structures. The abscissa and the ordinate list the replaced A and X element, respectively. A check mark indicates that this combination has a thermodynamically stable range in the pressure range of 50-400 GPa with respect to decomposition into the binary hydrides and the elemental phases, while a cross means it has not. Red check marks denote combinations that are predicted in this article and the green ones those that were already discovered by other researchers.

We constructed a series of ternary AXH_6 hydrides using A15 GaH_3 as the parent structure for atomic substitution. In A15 GaH_3 (Figure 1a), two Ga atoms form a body-centered cubic (bcc) lattice, and six H atoms occupy half of the tetrahedral interstices of the Ga lattice. If two Ga atoms in GaH_3 are replaced by two different X and A atoms,

then a $Pm\bar{3}$ (A15-type) AXH_6 structure (Figure 1b) is formed. Among them, Li, Na, K, Rb, Cs, Mg, Ca, Sr, Ba, Sc, and Y atoms were considered for A and Si, Ge, Sn, Pb, P, As, Sb, Bi, S, Se, and Te atoms for X. We performed a preliminary screening by analyzing the thermodynamic stability of the considered A15-type AXH_6 compounds with respect to decomposition into the binary hydrides and the elemental phases. As shown in Figure 1c, besides the already proposed A15-type $MgSiH_6$, $MgGeH_6$ and $LiPH_6$ systems, among the considered 121 combinations six new A15-type compounds ($MgPH_6$, $MgAsH_6$, $CaSbH_6$, $CaSnH_6$, $NaSbH_6$ and $ScSiH_6$) are predicted to be thermodynamically stable under pressure with respect to decomposition into the binary hydrides and solid elemental phases. Subsequently, crystal structural prediction combined with DFT calculations have been performed on the six new AXH_6 compounds to search for their most stable structures under pressure. The results show that the A15-type structure is indeed the most stable geometry for the AXH_6 stoichiometry in the pressure range of 50-300 GPa. Next, we will consider the electronic structures and properties of the $MgPH_6$, $MgAsH_6$, $CaSbH_6$, $CaSnH_6$, $NaSbH_6$ and $ScSiH_6$ phases in the A15-type structure.

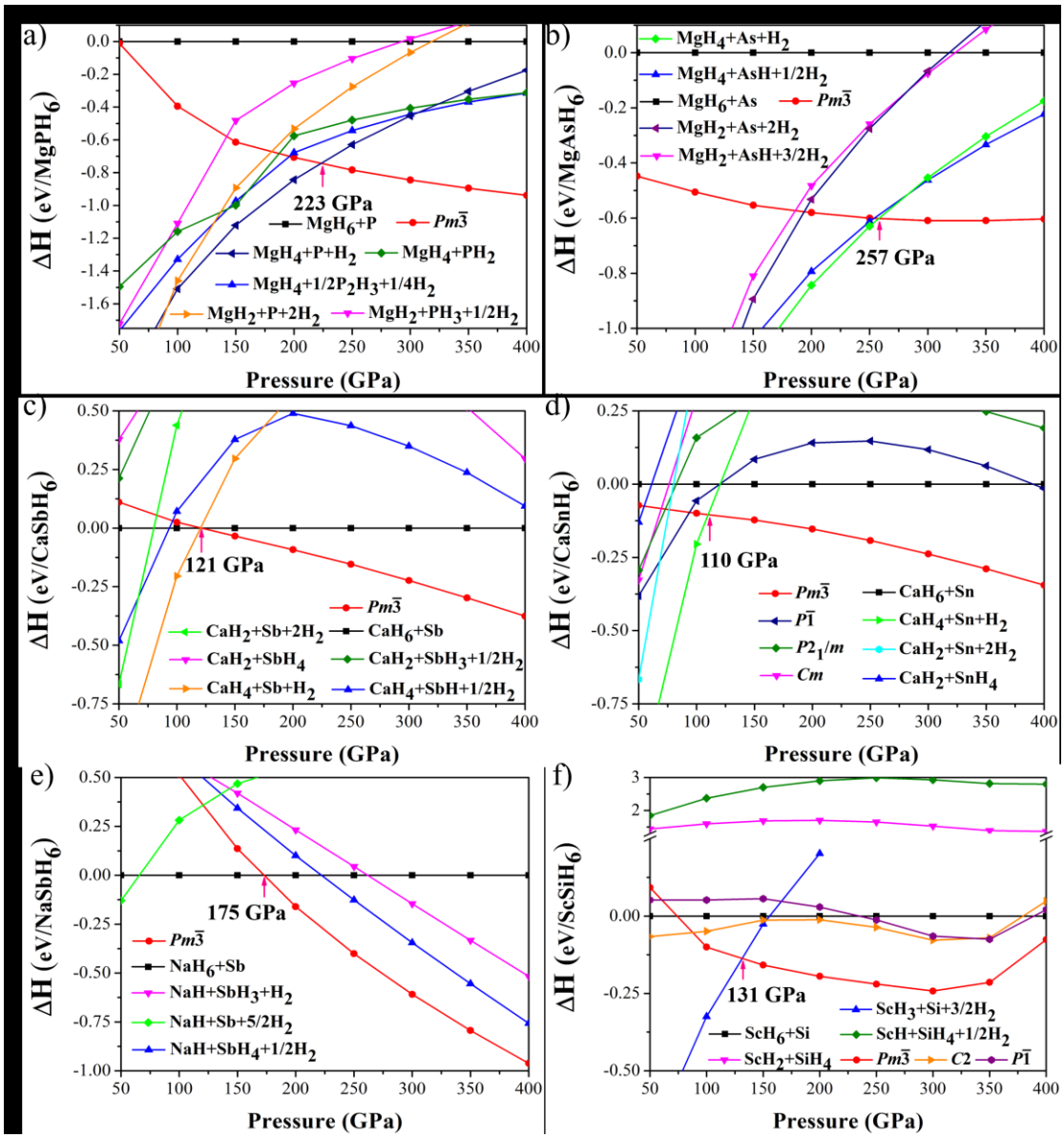

Figure 2: Relative enthalpies (ΔH) of the considered AXH_6 compounds with respect to decomposition into the listed binary hydrides and the elemental phases from 50 to 400 GPa. Results presented from (a) to (f) for $MgPH_6$, $MgAsH_6$, $CaSbH_6$, $CaSnH_6$, $NaSbH_6$ and $ScSiH_6$. The arrows point to the pressures where the ternaries are predicted to be thermodynamically stable. The following structures were considered for the binary hydrides: *P*63/*mmc* and *P*6/*mmm* for CaH_2, *I*4/*mmm* and *Cmcm* for CaH_4, *Im*$\bar{3}$*m* for CaH_6, *Pnma* and *P*6$_3$/*mmc* for MgH_2, *Cmcm* for MgH_4, *Im*$\bar{3}$*m* for MgH_6, *P.0m*$\bar{3}$*m* for NaH, *Pm*$\bar{3}$*m* for NaH_6, *Fm*$\bar{3}$*m* and *Cmcm* for ScH, *P*6/*mmm* for ScH_2, *Fm*$\bar{3}$*m* for ScH_3, *Cmcm*, *P*63/*mmc* and *Im*$\bar{3}$*m* for ScH_6, *Pnma* for SbH, *Pmmn* for SbH_3, *P*6$_3$/*mmc* for SbH_4, *Ama*2 and *P*6$_3$/*mmc* for SnH_4, *C*2/*m* for PH_3, P2$_1$/c for PH_2, *P*2$_1$/*m* for P_2H_3, *Fdd*2, *I*4$_1$/*a*, *Pbcn* and *C*2/*c* for SiH_4 and *Cmcm* for AsH. For the elemental solids we considered the following structures, *Pm*$\bar{3}$*m*, *P*6/*mmm* and *Imma* for P, *Im*$\bar{3}$*m* for As and Sb, *Cmca* and *Fm*$\bar{3}$*m* for Si, *Im*$\bar{3}$*m* and *P*6$_3$/*mmc* for Sn and *P*6$_3$/*m*, *C*2/*c* and *Cmca* for H_2.

To explore the range of thermodynamical stability of the six new A15-type AXH_6 compounds under pressure, the relative enthalpies with respect to the corresponding

constituent components, binary hydrides [30-40], elemental A or X phases [41-49] and solid H_2 [50, 51] are presented in Figure 2 and Figure S1 in the Supporting Information. It can be clearly seen that almost all of them are thermodynamically stable with respect to the elemental phases in the considered pressure range, while $MgPH_6$ is only unstable in a very narrow pressure range of 50-60 GPa. Interestingly, $CaSnH_6$ is thermodynamically stable at the lowest pressure of 110 GPa, and $CaSbH_6$, $ScSiH_6$, and $NaSbH_6$ have slightly higher pressures of stabilization, 121, 131 and 175 GPa, respectively. These four A15-type AXH_6 phases are thermodynamically stable at much lower pressures than the previously predicted $LiPH_6$, $MgSiH_6$ and $MgGeH_6$ compounds. However, $MgPH_6$ and $MgAsH_6$ become thermodynamically stable above much higher pressures of 223 and 257 GPa, respectively.

To study the dynamical stability of the six new A15-type AXH_6 structures, phonon spectra calculations were carried out in a much wider pressure range corresponding to thermodynamical stability. No imaginary frequencies in the phonon spectra suggests that they are all dynamically stable, as shown in Figure S2 in the Supporting Information. Moreover, these compounds can be dynamically stable to much lower pressures than those encompassing the range of thermodynamical stability, as shown in Figures S3-5. $CaSbH_6$, $CaSnH_6$ and $ScSiH_6$ can be dynamically stable at pressures as low as 41, 71 and 86 GPa, respectively, while the lowest dynamically stable pressures for $MgPH_6$, $MgAsH_6$ and $NaSbH_6$ are 133, 104 and 162 GPa, respectively. It can be clearly seen that $CaSnH_6$ is thermodynamically stable at the lowest pressure of 110 GPa, and is also dynamically stable at a relatively low pressure of 71 GPa. Moreover, all the six A15-type AXH_6 compounds can be dynamically stable at much lower pressures than the previously predicted $LiPH_6$, $MgSiH_6$ and $MgGeH_6$.

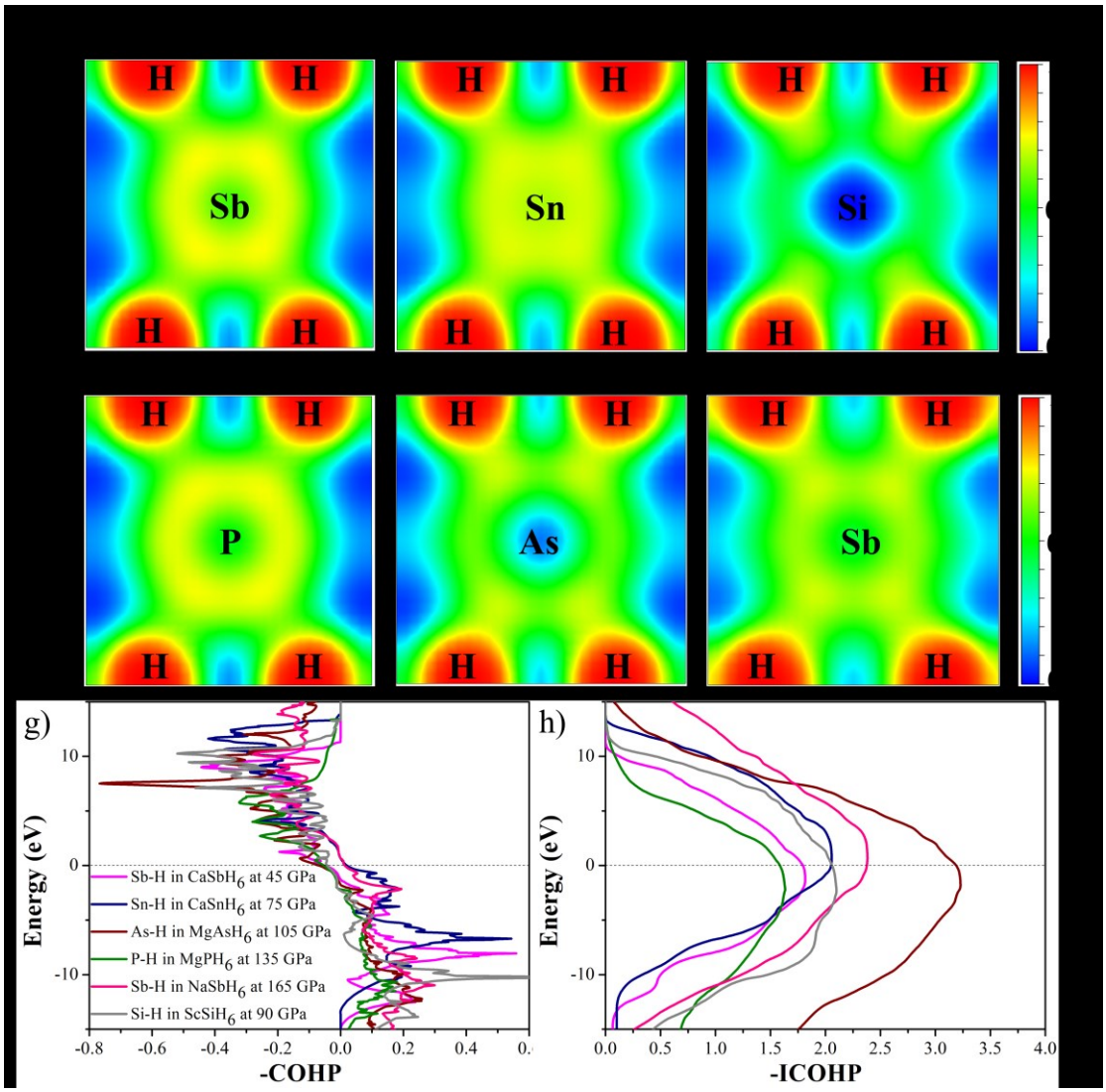

Figure 3: (a)-(f) The calculated electron localization function (ELF) on X-H planes for $Pm\bar{3}$ $CaSbH_6$, $CaSnH_6$, $ScSiH_6$, $MgPH_6$, $MgAsH_6$ and $NaSbH_6$ at 45, 75, 90, 135, 105 and 165 GPa, respectively. (g) and (h) are the calculated -COHP (crystal orbital Hamilton population) and its integration (-ICOHP) for X-H at different pressures.

In order to understand the chemical bonding of the six new A15-type AXH_6 phases, electron localization functions (ELF) were calculated. [52, 53], as shown in Figure 3a-3f and Figure S6-S7. Electrons are mainly concentrated around H atoms and an obvious elongation toward the X atoms appears (Figure S6). The ELF values between X and H atoms are 0.66, 0.68, 0.69, 0.66, 0.68 and 0.6 for $CaSbH_6$, $CaSnH_6$, $MgPH_6$, $MgAsH_6$, $NaSbH_6$ and $ScSiH_6$, respectively, indicating the weak covalent X-H bonds. The ELF values between Si and H atoms are relatively low, indicating that the Si-H bonds are weaker than other X-H bonds. Therefore, XH_{12} units are formed in these compounds.

In all AXH_6 compounds, the ELF values at the center of the shortest A-H distances are close to zero, indicating an ionic character for A-H bonds, see Figure S7. There are no H-H bonds from the ELF results.

For a deeper understanding of the bonding, we also calculated the Crystal Orbital Hamilton Population (COHP) and its integrated ICOHP projected onto A-H and X-H pairs in AXH_6 at different pressures. Positive and negative -COHP indicate bonding and antibonding interactions, respectively. The ICOHP up to the Fermi level can describe the atom pair interaction strength. It can be clearly seen from Figure 3, Figure S6 and Table S1 that the corresponding -ICOHPs at the Fermi level for X-H bonds in A15 AXH_6 are indeed much smaller than the typically covalent Si-H, Sn-H and P-H bonds in SiH_4, SnH_4 and PH_2 at different pressures. However, the -ICOHPs for all the X-H bonds in A15 AXH_6 are larger than or at least comparable to that of 1.61 for H-H bonds in clathrate LaH_{10}. Due to the weak covalent bonds in LaH_{10}, the X-H bonds in A15 AXH_6 might also be weak covalent bonds. Interestingly, the -ICOHP value of As-H in $MgAsH_6$ at 105 GPa is comparable to that of H-S in H_3S at 200 GPa, indicating the relatively strong covalent bond for As-H in $MgAsH_6$. The values of -ICOHP for the A-H pairs are much smaller than that for the X-H pairs, meaning no covalent bonds for the A-H pairs. In summary, X atoms in AXH_6 tend to form weak covalent bonds with the surrounding 12 H atoms, which is different from the ionic character observed in $Pm\bar{3}n$ GaH_3. Some hydrides with covalent bonds have been predicted and measured to be good superconductors under pressure[54]. For example, $Im\bar{3}m$ H_3S with S-H covalent bonds was observed to have a T_c of 203 K at 200 GPa [55] and $Pa\bar{3}$ $CaBH_6$ was estimated to have a T_c of 119 K at 300 GPa, due to strong B-H covalent bond stretching vibrations.[56] The design idea to form covalent bonds based on the A15-type structure leads us to a possible path to high-temperature superconducting ternary hydrides.

Bader charge calculations [57] are performed to determine the number of electrons transferred in the six new A15-type AXH_6. As shown in Table S2 and S3, H atoms

accept electrons from both A and X atoms in AXH_6. With increasing pressure, the number of electrons transferred from the A atoms decreases, while that from the X atoms increases. Our calculations reveal that the A15-type structure with the AXH_6 stoichiometry is stable when the sum of the formal valence on the non-hydrogen elements is seven ($MgPH_6$, $MgAsH_6$, $CaSbH_6$ and $ScSiH_6$). In A15 Ga_2H_6 and Al_2H_6, A15-type $LiPH_6$, $MgSiH_6$ and $MgGeH_6$, the sum of the chemical valences of the two non-hydrogen elements is six. Therefore, ternary hydrides with the AXH_6 stoichiometry seems to be stable in the A15-type structure under pressure when the sum of the chemical valences of the two non-hydrogen elements is six or seven. This rule can open a new route for the design of ternary hydrogen-rich compounds with the A15-type structure

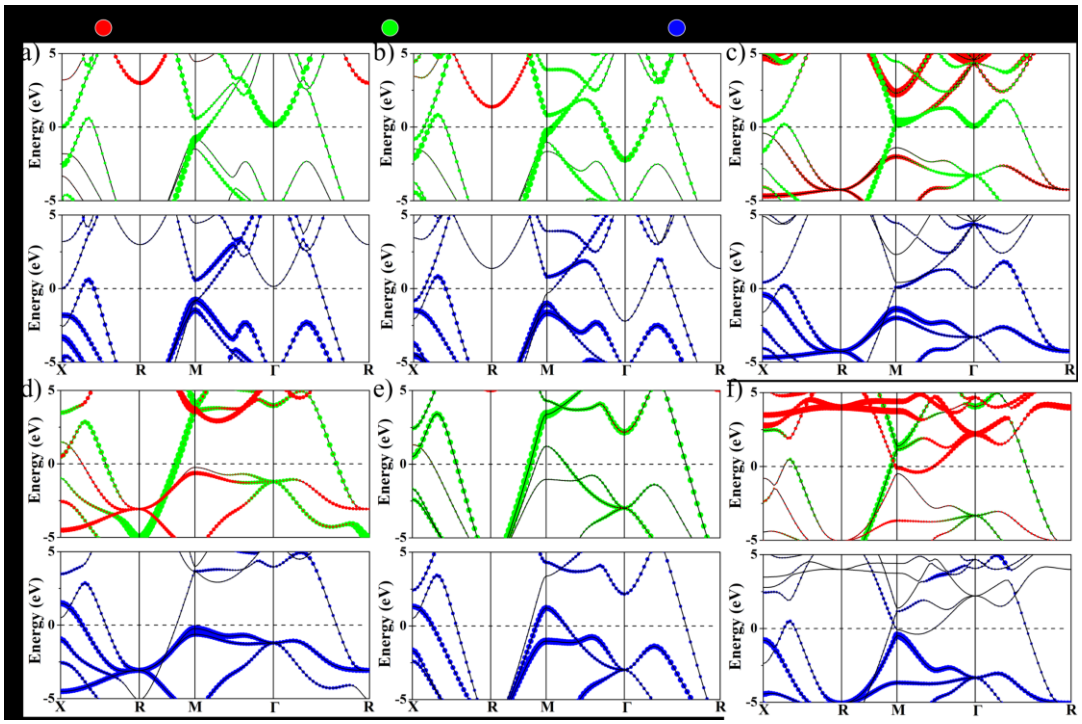

Figure 4: Electronic band structures and their projection on A, X and H atoms for (a) $MgPH_6$, (b) $MgAsH_6$, (c) $CaSbH_6$, (d) $CaSnH_6$, (e) $NaSbH_6$ and (f) $ScSiH_6$ at 135, 105, 45, 75, 165 and 90 GPa, respectively. (The radii of the circles are proportional to the weights of the projections to the corresponding atoms)

To further study the electronic properties of the six new A15-type AXH_6 compounds, their electronic band structure and their projections on the A, X and H atoms, and density of states (DOS) were calculated, as shown in Figures 4 and S8. The electronic DOS at the Fermi level (E_f) indicates that all AXH_6 compounds are metallic.

For $MgPH_6$, $MgAsH_6$, and $NaSbH_6$, the energy bands crossing the Fermi level are mainly characterized by H and X character, while for $CaSbH_6$, $CaSnH_6$ and $ScSiH_6$, all the atoms contribute comparably the DOS at E_f. For $CaSnH_6$ and $NaSbH_6$, the flat-steep band features are obvious and are distributed along *R-M* (steep band) and *M-Γ* (flat band) directions near the Fermi level, respectively. It has been postulated that flat-steep band features often beneficial for superconductivity[58]. The contribution of H atoms to the DOS at the Fermi level is significant for these AXH_6 hydrides, and it dominates the DOS at the Fermi level in $MgPH_6$, $CaSbH_6$, $CaSnH_6$ and $NaSbH_6$. This implies that these AXH_6 hydrides may be potential high-T_c superconductors.

Phase ($Pm\bar{3}$)	DSP (GPa)	TSPR (GPa)	λ	ω_{log} (K)	T_c (K) μ*=0.1-0.13 McMillan	T_c (K) μ*=0.1 Eliashberg
GaH_3($Pm\bar{3}n$)	84	160-400	1.67	857	126-114	154
$CaSbH_6$	45	121-400	1.48	579	65-59	—
$CaSnH_6$	75	110-400	1.32	532	53-48	—
$MgPH_6$	135	223-400	2.4	520	111-99	148
	200	223-400	1.06	1147	87-76	—
$MgAsH_6$	105	257-400	1.96	409	85-77	121
	150	257-400	0.93	1052	65-55	—
$NaSbH_6$	165	175-400	2.20	452	94-84	118
	200	175-400	0.91	1075	65-54	—
$ScSiH_6$	90	131-400	1.73	659	106-96	116
	150	131-400	0.90	1145	67-56	—
$LiPH_6$ [20]	200	250-400	1.62	1119	167-150	—
$MgSiH_6$ [18]	250	275-400	0.96	974	63-53	—
$MgGeH_6$ [19]	200	200-400	1.16	773	67(μ*=0.1)	—

Table 1: The calculated dynamically stable pressure (DSP), the lowest thermodynamically stable pressure range (TSPR), electron-phonon coupling (EPC) parameter λ, phonon logarithmic average frequency ω_{log} and critical temperature T_c (μ*=0.1-0.13) from the Allen-Dynes modified McMillan equation and calculated via solution of the Eliashberg equations for $Pm\bar{3}n$ GaH_3 and $Pm\bar{3}$ AXH_6 compounds. (The T_c values are obtained using the McMillan equation with the strong-coupling and shape corrections when $\lambda > 1.5$).

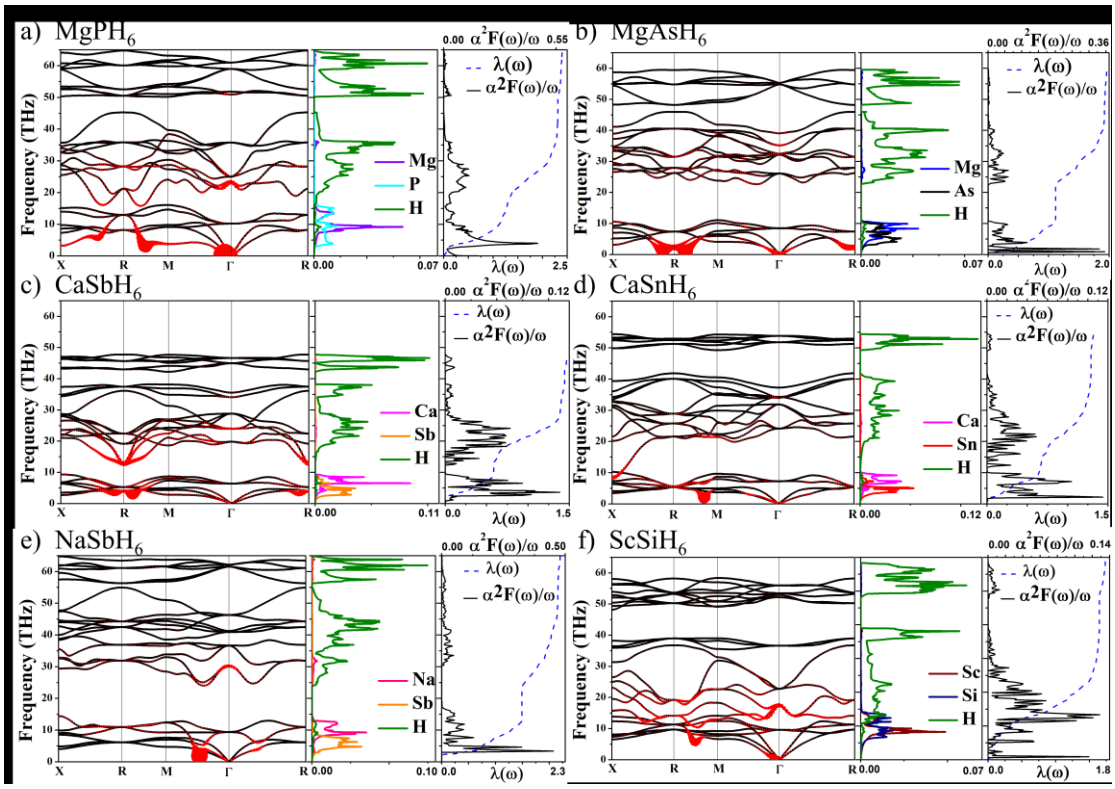

Figure 5: The calculated phonon dispersion curves (the area of the red circles is proportional to the EPC strength), projected phonon density of states, the Eliashberg phonon spectral function $\alpha^2F(\omega)/\omega$ and its integral $\lambda(\omega)$ for different AXH_6 compounds. From (a) to (f), $MgPH_6$, $MgAsH_6$, $CaSbH_6$, $CaSnH_6$, $NaSbH_6$ and $ScSiH_6$ are represented.

Considering their promising electronic properties mentioned above, the superconducting properties of the six new A15-type AXH_6 compounds are explored. The phonon dispersion curves, projected phonon density of states, the Eliashberg phonon spectral function $\alpha^2F(\omega)/\omega$ and its integral $\lambda(\omega)$ for the AXH_6 compounds are calculated at around the lowest dynamically stable pressures, as shown in Figure 5. Low-frequency branches (0-15 THz) are mainly associated with the vibrations of both A and X atoms, while the higher-frequency branches (above 15 THz) are dominated by the light H atoms. For all AXH_6 compounds the EPC has two main contributions, low-frequency modes associated to non-hydrogen vibrations and medium-frequency ones related to H vibrations. For example, in $CaSbH_6$ the contribution to λ of vibrations related to Ca and Sb atoms in the range of 3-8 THz accounts for 36% of the total value, while the contribution related to vibrations of H atoms in the range of 18-30 THz accounts for 47% of the total value. In the case of $CaSnH_6$, the contribution to $\boldsymbol{\lambda}$ of the vibrations related to Ca and Sn atoms in the range of 3-8 THz accounts for 39% of the

total value, while that of the vibrations related to H atoms in the range of 18-30 THz accounts for 36% of the total value. For $MgXH_6$ and $NaSbH_6$, the contribution to λ of the vibrations related to non-hydrogen atoms is also comparable to that of vibrations related to H atoms. However, for $ScSiH_6$, the contribution to λ of vibrations related to H atoms in the range of 11-24 THz reaches to 66%, which is much higher than that of vibrations related to Sc and Si atoms in the range of 3-11 THz (17%). To further explore the origin of superconductivity, we analyze the distribution of the EPC strength on different phonon modes. Interestingly, they present a phonon softening, where there is large electron-phonon coupling associated. However, the contribution to superconductivity from softened phonons is not significant, because even though it enhances λ, its small contribution to ω_{log} makes T_c decrease. For medium-frequency phonons related to H vibrations, they have a large contribution to λ and also make a significant contribution to ω_{log}, having, therefore, an important contribution to enhance T_c. However, high-frequency phonons, also related to H vibrations, present a small electron-phonon coupling, so that they almost do not have contribute to rise T_c. In order to further understand the phonon vibration mode of softening areas, we calculated the eigenvectors of the soft phonon modes at q = (0.5 0.5 0.42), taking $Pm\bar{3}$ $CaSbH_6$ as an example at 45 GPa as shown in Figure S9. The results show that the vibration modes of phonon softening region are mainly motions of the H atoms and partially the Ca atoms.

Next, we have estimated the T_c values of these six AXH_6 compounds at around the minimum pressures required for dynamic stability using the Allen-Dynes modified McMillan equation. The calculated results are shown in Table 1. For $CaSbH_6$ and $CaSnH_6$, the calculated EPC constants λ are 1.48 and 1.32 and the logarithmic average phonon frequency,ω_{log} , are 579 K and 532 K, leading to T_c values of 65 and 53 K with μ^* = 0.1 at 45 and 75 GPa, respectively. By numerically solving the Eliashberg equation, the T_cs of these compounds were enhanced to 85 and 70 K, respectively. For $MgPH_6$, $MgAsH_6$, $NaSbH_6$ and $ScSiH_6$, their λ reach 2.4, 1.96, 2.2 and 1.73 at 135, 105, 165 and 90 GPa, respectively, which are larger than that of $CaXH_6$. Since λ exceeds 1.5, better estimates can be obtained by considering the strong-coupling and shape

corrections ($f1$ and $f2$) approximation, with estimated T_c values of 111, 85, 94 and 106 K with $\mu^* = 0.1$, respectively. By numerically solving the Eliashberg equation, the T_cs of these compounds were enhanced to 148, 121, 118 and 116 K, respectively. With the increase of pressure, λ decreases to 1.06, 0.93, 0.91 and 0.9 at 200, 150, 200 and 150 GPa for $MgPH_6$, $MgAsH_6$, $NaSbH_6$ and $ScSiH_6$, respectively. Therefore, the estimated T_c values decrease to 87, 65, 65 and 67 K, respectively, even though the ω_{log}s increase.

For comparison, the T_c results for A15 GaH_3 calculated at the lowest dynamically stable pressure of 84 GPa, and $LiPH_6$, $MgSiH_6$ and $MgGeH_6$, already calculated previously, are also listed in Table 1. GaH_3 has the highest T_c of 154 K at 84 GPa, and it might be a good candidate for future experimental synthesis. $LiPH_6$, $MgSiH_6$ and $MgGeH_6$ were predicted to have T_cs of 167, 63 and 67 K at 200, 250 and 200 GPa, respectively. It can be seen that our predicted ternary hydrides, $CaSbH_6$, $CaSnH_6$, $NaSbH_6$, and $ScSiH_6$ are thermodynamically stable at lower pressures than previously proposed $LiPH_6$, $MgSiH_6$ and $MgGeH_6$. Moreover, all the proposed six new ternary hydrides can be dynamically stable at much lower pressures, while still keeping the relatively high T_cs. For example, $CaSbH_6$ is dynamically stable at the lowest pressure of 45 GPa with a T_c of 65 K. $CaSnH_6$, which has the lowest thermodynamically stable pressure of 110 GPa among these hydrides, has a T_c of 53 K at 70 GPa. It is also worth mentioning that the newly predicted $MgPH_6$ and $MgAsH_6$ have the same A atoms as $MgSiH_6$ and $MgGeH_6$, but they have higher T_cs (148 and 121 K) at lower pressures (135 and 105 GPa), which might be attributed to the stronger P-H and As-H bonds.

4. Conclusion

Six new A15-type AXH_6 compounds ($MgPH_6$, $MgAsH_6$, $CaSbH_6$, $CaSnH_6$, $NaSbH_6$ and $ScSiH_6$) are designed by density functional theory calculations combined with structure searches and high throughput calculations on a particular structure type taking into consideration particular chemical substitutions. Thermodynamical stability, electronic properties, lattice dynamics, and superconductivity of these compounds are systematically investigated. Enthalpy calculations with respect to decomposition into various binary hydrides provides a reference for potential experimental synthesis.

$CaSnH_6$ has the lowest thermodynamically stable pressure of 110 GPa. Furthermore, all the six new A15-type AXH_6 compounds are dynamically stable at much lower pressures than in previously predicted $LiPH_6$, $MgSiH_6$ and $MgGeH_6$. Interestingly, $CaSbH_6$, $CaSnH_6$ and $ScSiH_6$ can be dynamically stable at pressures below 100 GPa. X-H weak covalent bonds are predicted in these AXH_6 compounds and the A atoms act as chemical precompressors and electron donors. The sum of chemical valences of the two non-hydrogen elements of these stable hydrides is six or seven. Remarkably, all these ternary hydrides are predicted to be good superconductors. $CaSbH_6$, $CaSnH_6$ and $ScSiH_6$ have T_cs of 65, 53 and 116 K at 45, 75 and 90 GPa, while $MgPH_6$ has the highest T_c up to 148 K at 135 GPa. These high T_cs are due to the formation of strong X-H covalent bonds and softened phonons. Our work enriches the study of ternary hydrides with the A15 structure-type and will stimulate the design of other ternary hydrides with high-symmetry structures at lower pressures but with relatively high T_cs.

Credit author statement

Guoying Gao initiated the project. Xudong Wei and Guoying Gao performed the calculations and wrote the manuscript. Guoying Gao, Xudong Wei, Aitor Bergara, Eva Zurek, Linyan Wang, Xiaokuan Hao, Xiaoxu Song, Peifang Li, Lin Wang, and Yongjun Tian analyzed the data and revised the manuscript.

Declaration of competing interest

The authors declare that they have no known competing financial interests or personal relationships that could have appeared to influence the work reported in this paper.

Acknowledgements

This work was supported by Natural Science Foundation of China (Grant Nos. 52022089, 11874076, 52090020, 2022YFA1402300, 5288102, 11964026). P.F. Li thanks Science and Technology Leading Talents and Innovation Team Building Projects of Inner Mongolia Autonomous Region (GXKY22060). A.B. acknowledges financial support from the Spanish Ministry of Science and Innovation (Grant No. FIS2019-

105488GB-I00) and the Department of Education, Universities and Research of the Basque Government and the University of the Basque Country (IT1707-22). E. Z. acknowledges the National Science Foundation (DMR-2136038) for financial support.

Appendix A. Supplementary data

The following is the Supplementary data to this article:

Supporting Information is available from the appendix or from the author.

References:

[1] G.F. Hardy, J.K. Hulm, Superconducting Silicides and Germanides, Physical Review 89(4) (1953) 884-884.

[2] J.H.W.a.W.A.R. L.R. Testardi, Superconductivity with onset above 23° K in Nb_3Ge sputtered films, Solid State Communications 15(1) (1974) 1-4.

[3] J.R. Gavaler, M.A. Janocko, C.K. Jones, Preparation and properties of high-T_c Nb-Ge films, J. Appl. Phys. 45(7) (1974) 3009-3013.

[4] Z. Fisk, G.W. Webb, Saturation of the High-Temperature Normal-State Electrical Resistivity of Superconductors, Physical Review Letters 36(18) (1976) 1084-1086.

[5] G.S. Knapp, S.D. Bader, Z. Fisk, Phonon properties of A−15 superconductors obtained from heat-capacity measurements, Physical Review B 13(9) (1976) 3783-3789.

[6] S. Païdassi, J. Spitz, J. Besson, Chemical vapor deposition of Nb_3Ge on continuous stainless-steel tapes, Applied Physics Letters 33(1) (1978) 105-107.

[7] J.G. Bednorz, K.A. Müller, Possible high T_c superconductivity in the Ba-La-Cu-O system, Z. Physik B - Condensed Matter 64(2) (1986) 189-193.

[8] A.Y. Ganin, Y. Takabayashi, Y.Z. Khimyak, S. Margadonna, A. Tamai, M.J. Rosseinsky, K. Prassides, Bulk superconductivity at 38 K in a molecular system, Nat Mater 7(5) (2008) 367-371.

[9] F.H.E.a.W.H.Z.-A. R.N.R.Mulford, A New Form of Uranium Hydride1, J. Am. Chem. Soc. 76 (1954) 297-298.

[10] C.J. Pickard, R.J. Needs, Metallization of aluminum hydride at high pressures: A first-principles study, Phys. Rev. B 76(14) (2007) 144114.

[11] I. Goncharenko, M.I. Eremets, M. Hanfland, J.S. Tse, M. Amboage, Y. Yao, I.A. Trojan, Pressure-induced hydrogen-dominant metallic state in aluminum hydride, Phys. Rev. Lett. 100(4) (2008) 045504.

[12] G. Gao, H. Wang, A. Bergara, Y. Li, G. Liu, Y. Ma, Metallic and superconducting gallane under high pressure, Phys. Rev. B 84(6) (2011) 064118.

[13] H. Xie, W. Zhang, D. Duan, X. Huang, Y. Huang, H. Song, X. Feng, Y. Yao, C.J. Pickard, T. Cui, Superconducting zirconium polyhydrides at moderate pressures, J. Phys. Chem. Lett. 11(3) (2020) 646-651.

[14] G. Gao, R. Hoffmann, N.W. Ashcroft, H. Liu, A. Bergara, Y. Ma, Theoretical study of the ground-state structures and properties of niobium hydrides under pressure, Physical Review B 88(18) (2013) 184104.

[15] G. Liu, S. Besedin, A. Irodova, H. Liu, G. Gao, M. Eremets, X. Wang, Y. Ma, Nb-H system at high pressures and temperatures, Physical Review B 95(10) (2017) 104110.

[16] J. Ying, X. Li, E. Greenberg, V.B. Prakapenka, H. Liu, V.V. Struzhkin, Synthesis and stability of tantalum hydride at high pressures, Physical Review B 99(22) (2019) 224504.

[17] G. Gao, L. Wang, M. Li, J. Zhang, R.T. Howie, E. Gregoryanz, V.V. Struzhkin, L. Wang, J.S. Tse, Superconducting binary hydrides: Theoretical predictions and experimental progresses, Materials Today Physics 21 (2021) 100546.

[18] Y. Ma, D. Duan, Z. Shao, H. Yu, H. Liu, F. Tian, X. Huang, D. Li, B. Liu, T. Cui, Divergent synthesis routes and superconductivity of ternary hydride $MgSiH_6$ at high pressure, Physical Review B 96(14) (2017) 144518.

[19] Y. Ma, D. Duan, Z. Shao, D. Li, L. Wang, H. Yu, F. Tian, H. Xie, B. Liu, T. Cui, Prediction of superconducting ternary hydride $MgGeH_6$: from divergent high-pressure formation routes, Phys Chem Chem Phys 19(40) (2017) 27406-27412.

[20] Z. Shao, D. Duan, Y. Ma, H. Yu, H. Song, H. Xie, D. Li, F. Tian, B. Liu, T. Cui, Ternary superconducting cophosphorus hydrides stabilized via lithium, npj Computational Materials 5(1) (2019) 238-245.
[21] J.L. Y.Wang, L.Zhu, and Y.Ma,, CALYPSO: a method for crystal structure prediction, Comput. Phys. Commun. 183 (2012) 2063.
[22] Y. Wang, J. Lv, L. Zhu, Y. Ma, Crystal structure prediction via particle-swarm optimization, Physical Review B 82(9) (2010) 094116.
[23] G.K.a.J. Furthmüller, Efficient iterative schemes for ab initio total-energy calculations using a plane-wave basis set, Phys. Rev. B 54 (1996) 11169-11186.
[24] J.P. Perdew, J.A. Chevary, S.H. Vosko, K.A. Jackson, M.R. Pederson, D.J. Singh, C. Fiolhais, Atoms, molecules, solids, and surfaces: Applications of the generalized gradient approximation for exchange and correlation, Phys Rev B Condens Matter 46(11) (1992) 6671-6687.
[25] P.E. Blochl, Projector augmented-wave method, Phys Rev B Condens Matter 50(24) (1994) 17953-17979.
[26] A. Togo, F. Oba, I. Tanaka, First-principles calculations of the ferroelastic transition between rutile-type and $CaCl_2$-type SiO_2 at high pressures, Physical Review B 78(13) (2008) 134106.
[27] S.B. P. Giannozzi, N. Bonini, M. Calandra, R. Car, C., D.C. Cavazzoni, G. L. Chiarotti, M. Cococcioni, and I., Dabo, QUANTUM ESPRESSO: a modular and open-source software project for quantum simulations of materials, J. Phys.: Condens. Matter 21 (2009) 395502.
[28] P.B. Allen, R.C. Dynes, Transition temperature of strong-coupled superconductors reanalyzed, Phys. Rev. B 12(3) (1975) 905-922.
[29] G. Eliashberg, INTERACTIONS BETWEEN ELECTRONS AND LATTICE VIERA TIONS IN A SUPERCONDUCTOR, Sov. Phys. JETP 11 (1960) 696.
[30] Y. Fu, X. Du, L. Zhang, F. Peng, M. Zhang, C.J. Pickard, R.J. Needs, D.J. Singh, W. Zheng, Y. Ma, High-pressure phase stability and superconductivity of pnictogen hydrides and chemical trends for compressed hydrides, Chem. Mater. 28(6) (2016) 1746-1755.
[31] H. Liu, Y. Li, G. Gao, J.S. Tse, I.I. Naumov, Crystal structure and superconductivity of PH_3 at high pressures, J. Phys. Chem. C 120(6) (2016) 3458-3461.
[32] M. Martinez-Canales, A.R. Oganov, Y. Ma, Y. Yan, A.O. Lyakhov, A. Bergara, Novel structures and superconductivity of silane under pressure, Phys Rev Lett 102(8) (2009) 087005.
[33] G. Gao, A.R. Oganov, P. Li, Z. Li, H. Wang, T. Cui, Y. Ma, A. Bergara, A.O. Lyakhov, T. Iitaka, G. Zou, High-pressure crystal structures and superconductivity of Stannane (SnH_4), Proc. Natl. Acad. Sci. USA 107(4) (2010) 1317-1320.
[34] J.S. Tse, D.D. Klug, S. Desgreniers, J.S. Smith, R. Flacau, Z. Liu, J. Hu, N. Chen, D.T. Jiang, Structural phase transition in CaH_2 at high pressures, Phys. Rev. B 75(13) (2007) 134108.
[35] H. Wang, J.S. Tse, K. Tanaka, T. Iitaka, Y. Ma, Superconductive sodalite-like clathrate calcium hydride at high pressures, Proc. Natl. Acad. Sci. USA 109(17) (2012) 6463-6466.
[36] A.K. Mishra, T. Muramatsu, H. Liu, Z.M. Geballe, M. Somayazulu, M. Ahart, M. Baldini, Y. Meng, E. Zurek, R.J. Hemley, New Calcium Hydrides with Mixed Atomic and Molecular Hydrogen, The Journal of Physical Chemistry C 122(34) (2018) 19370-19378.
[37] D.C. Lonie, J. Hooper, B. Altintas, E. Zurek, Metallization of magnesium polyhydrides under pressure, Phys. Rev. B 87(5) (2013) 054107.
[38] P. Baettig, E. Zurek, Pressure-stabilized sodium polyhydrides: NaH(n) (n>1), Phys Rev Lett 106(23) (2011) 237002.

[39] X. Ye, R. Hoffmann, N.W. Ashcroft, Theoretical Study of Phase Separation of Scandium Hydrides under High Pressure, The Journal of Physical Chemistry C 119(10) (2015) 5614-5625.
[40] K. Abe, Hydrogen-rich scandium compounds at high pressures, Phys. Rev. B 96(14) (2017) 144108.
[41] H.-k.M.a.R.A. Sergiu Arapan, Prediction of incommensurate crystal structure in Ca at high pressure, Proc. Natl. Acad. Sci. USA 105 (2008) 20627-20630.
[42] G.G. Peifang Li, Yanchao Wang, and Yanming Ma, Crystal Structures and Exotic Behavior of Magnesium under Pressure, J. Phys. Chem. C 114 (2010) 21745-21749.
[43] M. Hanfland, I. Loa, K. Syassen, Sodium under pressure: bcc to fcc structural transition and pressure-volume relation to 100 GPa, Physical Review B 65(18) (2002) 184109.
[44] L.F.L. Eugene Gregoryanz, Malcolm I. McMahon, Christophe Guillaume, Richard J. Nelmes, Mohamed Mezouar, Structural Diversity of Sodium, Science 320 (2008) 1054-1057.
[45] M.I. McMahon, L.F. Lundegaard, C. Hejny, S. Falconi, R.J. Nelmes, Different incommensurate composite crystal structure for Sc-II, Physical Review B 73(13) (2006) 134102.
[46] S.-C. Zhu, X.-Z. Yan, S. Fredericks, Y.-L. Li, Q. Zhu, First-principles investigation of Sc-III/IV under high pressure, Physical Review B 98(21) (2018) 214116.
[47] H. Katzke, P. Tolédano, Displacive mechanisms and order-parameter symmetries for the A7-incommensurate-bcc sequences of high-pressure reconstructive phase transitions in Group Va elements, Physical Review B 77(2) (2008) 024109.
[48] H. Giefers, E.A. Tanis, S.P. Rudin, C. Greeff, X. Ke, C. Chen, M.F. Nicol, M. Pravica, W. Pravica, J. Zhao, A. Alatas, M. Lerche, W. Sturhahn, E. Alp, Phonon density of states of metallic Sn at high pressure, Phys Rev Lett 98(24) (2007) 245502.
[49] H. Katzke, U. Bismayer, P. Tolédano, Theory of the high-pressure structural phase transitions in Si, Ge, Sn, and Pb, Physical Review B 73(13) (2006) 134105.
[50] C.J. Pickard, R.J. Needs, Structure of phase III of solid hydrogen, Nature Physics 3(7) (2007) 473-476.
[51] H. Liu, H. Wang, Y. Ma, Quasi-Molecular and Atomic Phases of Dense Solid Hydrogen, The Journal of Physical Chemistry C 116(16) (2012) 9221-9226.
[52] A.D. Becke, K.E. Edgecombe, A simple measure of electron localization in atomic and molecular systems, The Journal of Chemical Physics 92(9) (1990) 5397-5403.
[53] O.J. A. Savin, J. Flad, O. K. Andersen, H. Preuss, and, H.G.v. Schnering, Electron Localization in Solid-state Structures of the Elements: the Diamond Structure, Angew. Chem. Int. Ed. 31 (1992) 187-188.
[54] B. Lilia, R. Hennig, P. Hirschfeld, G. Profeta, A. Sanna, E. Zurek, W.E. Pickett, M. Amsler, R. Dias, M.I. Eremets, C. Heil, R.J. Hemley, H. Liu, Y. Ma, C. Pierleoni, A.N. Kolmogorov, N. Rybin, D. Novoselov, V. Anisimov, A.R. Oganov, C.J. Pickard, T. Bi, R. Arita, I. Errea, C. Pellegrini, R. Requist, E.K.U. Gross, E.R. Margine, S.R. Xie, Y. Quan, A. Hire, L. Fanfarillo, G.R. Stewart, J.J. Hamlin, V. Stanev, R.S. Gonnelli, E. Piatti, D. Romanin, D. Daghero, R. Valenti, The 2021 room-temperature superconductivity roadmap, J Phys Condens Matter 34(18) (2022).
[55] M.I.E. A. P. Drozdov, I. A. Troyan, V. Ksenofontov and S. I. Shylin, Conventional superconductivity at 203 kelvin at high pressures in the sulfur hydride system, Nature 525 (2015) 73-76.
[56] S. Di Cataldo, W. von der Linden, L. Boeri, Phase diagram and superconductivity of calcium borohyrides at extreme pressures, Physical Review B 102(1) (2020).
[57] R. Bader, Atoms in Molecules: A Quantum Theory, (Oxford University Press, Oxford, 1994).
[58] A. Simon, Simon - Superconductivity and Chemistry, Angew. Chem. Int. Ed. (36) (1997) 1788.